

Hilbert phase analysis of the dynamics of a semiconductor laser with optical feedback

Wing-Shun Lam,^{1,2} Parvez N. Guzdar,² and Rajarshi Roy^{1,2,3}

¹*Department of Physics, University of Maryland, College Park, Maryland 20742*

²*IREAP, University of Maryland, College Park, Maryland 20742*

³*IPST, University of Maryland, College Park, Maryland 20742*

(Received 15 February 2002; published 27 February 2003)

The nonlinear dynamics of a semiconductor laser with an optical feedback is studied using Hilbert phase analysis, which reveals interesting facets of the nonlinear dynamical behavior, including the formation and interaction of external cavity modes with increasing external feedback. Here we report measurements on two illustrative cases with very different dynamics; the laser is first biased just near threshold, and then far above threshold. We observe 2π phase jumps at intervals that are multiples of the external cavity round-trip time, indicating the interaction and transfer of energy between external cavity modes.

DOI: 10.1103/PhysRevE.67.025604

PACS number(s): 42.65.Sf, 05.40.Ca, 05.45.Jn, 42.55.Px

A semiconductor laser with time-delayed optical feedback is one of the most interesting nonlinear dynamical systems in which the interplay of high-dimensional dynamics and noise can be studied. Depending on the amount of feedback and the pumping current, the laser operates in different dynamical regimes. When a laser biased very near threshold is subject to moderate feedback from a distant mirror, the output power drops to almost zero randomly, and then recovers [1]. These well separated, discrete events are called power dropouts. With higher pumping current and feedback, the laser dynamics changes to a coherence-collapse regime characterized by a breakdown of the coherence length from several meters to a few millimeters [2], and fast, chaotic fluctuations. In the last decade, there have been many studies of these various phenomena that attempt to provide a physical understanding of the system [3–17].

Theoretically, the laser system is often described by the Lang-Kobayashi equations [3], which are coupled delay-differential equations for the complex laser field and population inversion in the active region of the laser. The nonlinear dynamics leading to dropouts, described by the trajectory in the phase space spanned by the population inversion and the complex field phase shift for one round-trip time, is a well-understood mechanism based on the solution of the Lang-Kobayashi equations [6]. In communication theory, an informative way of extracting phase information from the time series of a real signal is provided by Hilbert transforms and the analytic signal introduced by Gabor [18]. The calculated Hilbert phase has been demonstrated to be a very powerful technique to discover valuable information from the original intensity data [19]—in particular, it can reveal interference effects and interactions between coupled modes that are involved in the time evolution of a dynamical system. Note that the nature of the Hilbert phase dynamics is distinct from the dynamics of the complex field phase.

For any real time series $I^{(r)}(t)$, such as the laser intensity, we can get the corresponding analytic signal $I(t) = I^{(r)}(t) + iI^{(i)}(t)$, where $I^{(i)} \equiv \pi^{-1} P \int_{-\infty}^{\infty} I^{(r)}(t') (t' - t)^{-1} dt'$ is the Hilbert transform of $I^{(r)}(t)$ and P is the principal value of the integral. Writing $I(t) = A(t)e^{i\phi_H(t)}$, where $A(t)$ is a real function, we get the Hilbert phase $\phi_H(t)$ of the real signal

$I^{(r)}(t)$. It is a phase that describes changes in the field envelope and it can be evaluated both from experiments and simulations.

In the experiment, a temperature controller is used to stabilize (to better than 0.01 K) a Fabry-Perot semiconductor laser (Sharp LT015MD) with an antireflection coating of $\approx 10\%$ reflectivity on one facet and a high reflection coating on the other facet. The light ($\lambda = 830$ nm) from the laser is reflected by a mirror placed at a distance of 45 cm from the antireflection-coated facet (external cavity round-trip time $\tau = 3$ ns). A beam splitter directs light onto a photodetector (New Focus Model 1554, 12 GHz bandwidth). The output of the photodetector is recorded by a digital oscilloscope (Tektronix TDS7104, 1 GHz bandwidth, 10 G samples per second) with resolution 100 ps. Different dynamical regimes of the laser are obtained for different levels of feedback strength and current.

First, we bias the laser at threshold, and introduce a moderate feedback that reduces the threshold current by about 5%. In Fig. 1(a), we see the well-known power dropout in the output light from the laser. The intensity fluctuates with a relatively large amplitude during the maximal output period, then abruptly drops to almost zero, followed by a gradual recovery, leading subsequently to another dropout event. The average intensity of the time series has been filtered out. The maximal output region shows characteristic intensity fluctuations that arise from a combination of feedback and the effect of spontaneous emission. In Fig. 1(b), we plot the Hilbert phase shift $\Delta\phi \equiv \phi_H(t) - \phi_H(t - \tau)$, for the one round-trip time τ vs time. The two regions in Fig. 1(a) are clearly distinguishable here. In the dropout region, the phase shift is zero. In the maximal output region, the phase shift has random jumps forming column structures with widths that are multiples of 3 ns, the round-trip time, and heights that are multiples of 2π . The zero phase shift in the dropout region is obvious because $I^{(r)}(t)$ is always negative such that $I(t) = I^{(r)}(t) + iI^{(i)}(t)$ always stays in the left half complex plane.

To discover the relationship between the intensity and the phase shift, the maximal output region during the period from $t = 341$ to 359 ns is examined in detail for which the

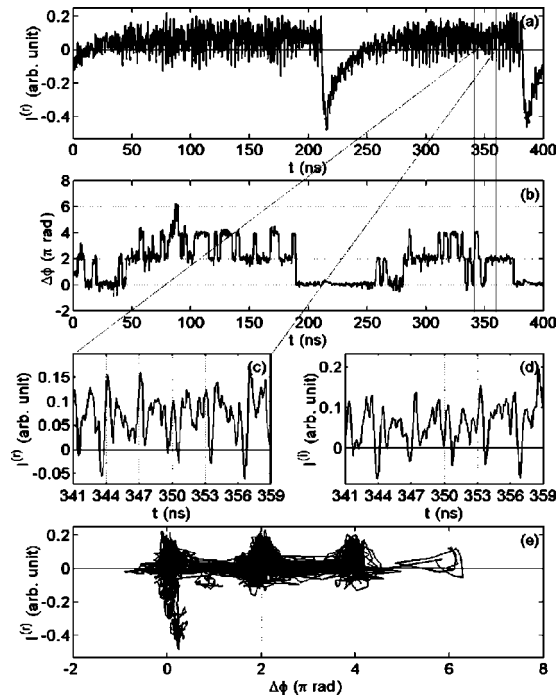


FIG. 1. (a) Intensity time series of the laser biased at threshold; (b) the corresponding Hilbert phase shift for one round trip of the external cavity; (c) detail of the real intensity time series; (d) the corresponding imaginary part of (c); (e) the trajectory of the laser in the phase space of the intensity vs Hilbert phase shift.

phase shift has three different values 0 , 2π , and 4π . Figures 1(c) and 1(d) show the real intensity time series and the corresponding imaginary part, respectively, during that period. We can see that in the interval 350–359 ns, $I^{(r)}(t)$ and $I^{(i)}(t)$ cross zero once every round-trip time $\tau=3$ ns with a lag between them, which corresponds to one revolution around the origin of the complex plane. This gives a 2π change in the Hilbert phase shift in this interval. If there is one period with two crossings of zero, both in the real part and the corresponding imaginary part, as occurs in the interval 341–344 ns in Figs. 1(c) and 1(d), then the phase shift will display a column with height 2π and width 3 ns on top of the 2π platform as seen in Fig. 1(b). If there are two consecutive periods with two crossings (of zero), then the width of the column will be 6 ns. On the other hand, if there is a full period without any crossing in the real part *or* imaginary part, as occurs in the interval 347–350 ns, then there will be a well with depth 2π and width 3 ns on the 2π platform [Fig. 1(b)]. Therefore, the Hilbert phase shift jumps randomly in multiples of 2π with widths that are multiples of τ . Whether the intensity crosses zero or not is controlled by the interference between and interaction of the external cavity modes. Consequently, the Hilbert phase captures the dynamics of the nonlinear interaction between the external cavity modes whose frequencies differ by $2\pi/\tau$.

In Fig. 1(e), we see the resulting multicluster structure with a cluster at zero phase shift, which corresponds to the dropout region. The zero-phase cluster thus identifies the dropout phenomenon, while those at integer multiples of 2π correspond to the existence and interaction of external cavity

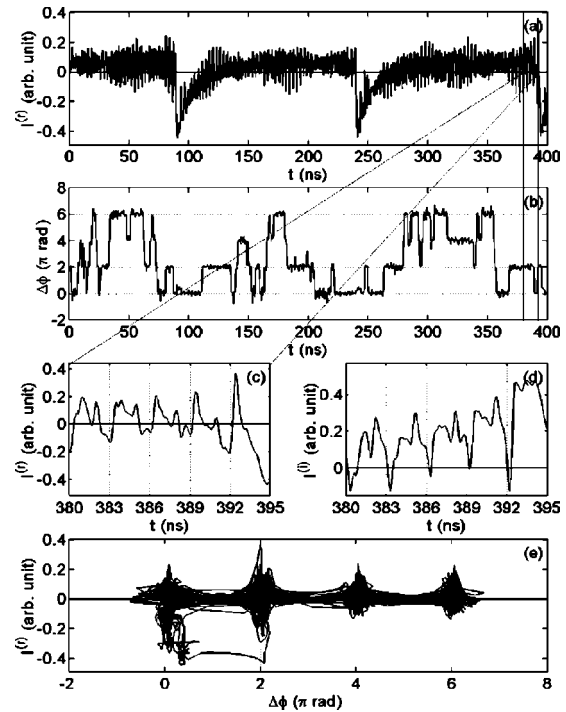


FIG. 2. (a) Simulated intensity time series of the laser with $P=1.01$ and $R=0.05$; (b) the corresponding Hilbert phase shift for one round trip; (c) detail of the real intensity time series; (d) the corresponding imaginary part of (c); (e) the trajectory of the laser in the phase space of the intensity vs Hilbert phase shift.

modes due to the optical feedback.

The above experimental results can be understood by integrating the Lang-Kobayashi equations given below [7,8],

$$\frac{dE}{dt} = \frac{1}{2}(1+i\alpha)G_{n,0}\sqrt{\frac{r_0}{r}}nE(t) + \kappa E(t-\tau)e^{-i\omega_0\tau} + F_E(t), \quad (1)$$

$$\frac{dn}{dt} = (P-1)\frac{N_{th}}{\tau_r} - \Gamma_n|E|^2 - n\left(\frac{1}{\tau_r} + G_{n,0}\sqrt{\frac{r_0}{r}}|E|^2\right), \quad (2)$$

using a standard fourth-order Runge-Kutta method. Here, $E(t)$ is the complex field; $n(t) \equiv [N(t) - N_{th}]$ is the difference between the carrier number at an arbitrary time and the threshold carrier number $N_{th} = 3.9 \times 10^8$; $\alpha = 5$ is the linewidth enhancement factor; $G_{n,0} = 21400 \text{ s}^{-1}$ and $r_0 = 0.32$ are the differential gain and facet power reflectivity for a laser with uncoated facet, respectively; $r = 0.1$ is the facet power reflectivity of a laser with an antireflection coating; $\kappa = (1-r)(R/r)^{1/2}/\tau_{in}$ is the feedback rate, where R is external mirror power reflectivity, $\tau_{in} = 3.9 \text{ ps}$ is the solitary laser pulse round-trip time; $\tau = 3.0 \text{ ns}$ is the external cavity round-trip time; ω_0 is the solitary laser frequency; $F_E(t)$ is the Langevin noise term, with $\langle F_E(t)F_E(t')^* \rangle = R_{sp}\delta(t-t')$, where $R_{sp} = 10^{14} \text{ s}^{-1}$ is the spontaneous emission rate; P is the ratio of pumping and threshold currents; $\tau_r = 1.1 \text{ ns}$ is the carrier recombination time; and $\Gamma_n = 1.1 \text{ ps}^{-1}$ is the photon decay rate. The constant value of $\omega_0\tau$ is taken to be a multiple of 2π for convenience. The equations are integrated

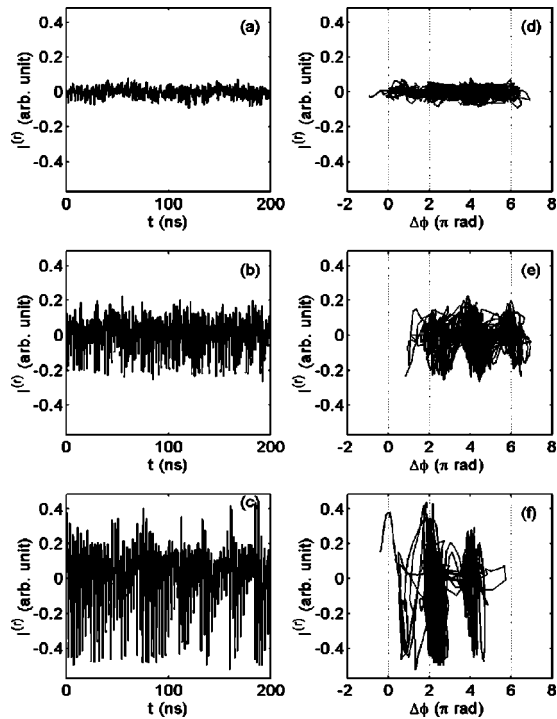


FIG. 3. (a), (b), and (c) Intensity time series of the laser pumped at 70 mA under feedback reducing the threshold current by 1%, 7.6%, and 12.3%, respectively; (d), (e), and (f) the corresponding trajectories of the laser in the phase space of intensity vs Hilbert phase shift.

with a time step of 0.5 ps from $t=0$ to $3 \mu\text{s}$ and we record only the last $2 \mu\text{s}$ in order to remove the transient behavior influenced by initial conditions. The original time series are then Fourier transformed and a low pass 1 GHz bandwidth filter is applied to simulate the digital oscilloscope electronics. We then repeat the Hilbert phase computation on the numerical intensity time series, similar to that for the experimental data.

In Fig. 2, we show the results from the simulation using Eqs. (1) and (2) with $P=1.01$ and $R=0.05$. As alluded to earlier, the spontaneous emission noise term is included since it is important near threshold. Its inclusion is essential to reproduce the shape and frequency of dropout events, and its magnitude is adjusted carefully to obtain agreement with experimental results. We obtain an intensity time series very similar to the experimental one [Fig. 2(a)]. The calculated Hilbert phase shift in Fig. 2(b) also shows the zero-phase-shift region and 2π columnar structure region. In Figs. 2(c) and 2(d), the real and imaginary parts of the analytic signal during which the phase shift has a well with depth 2π and width 3 ns show periodic behavior with period τ except the noncrossing zero in the imaginary part from 389 to 392 ns. The corresponding phase space in Fig. 2(e) shows different clusters at multiples of 2π . The overall agreement between the simulated behavior and the observed signal is excellent even though there are subtle differences.

In Figs. 3(a), 3(b), and 3(c), we display three intensity time series $I^{(r)}(t)$ for different feedback strengths, which reduce the threshold current by 1%, 7.6%, and 12.3% under a

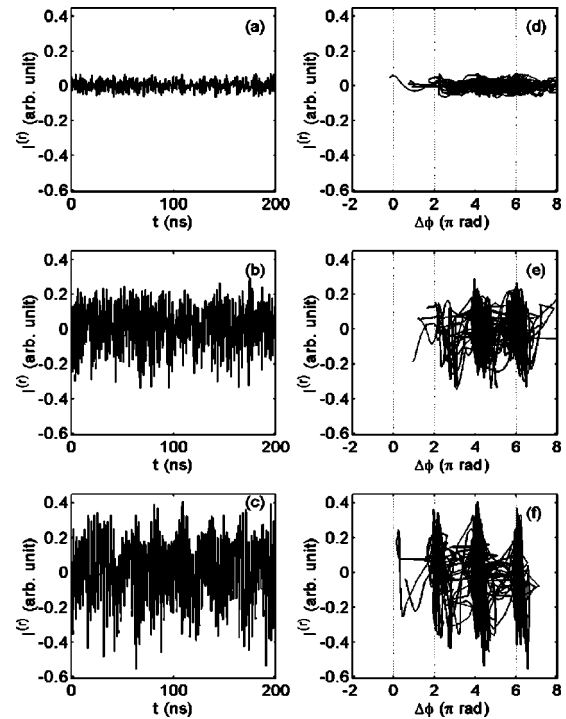


FIG. 4. (a), (b), and (c) Simulated intensity time series of the laser with $P=1.24$ and $R=0.01$, 0.076, and 0.123, respectively; (d), (e), and (f) the corresponding trajectories of the laser in the phase space of intensity vs Hilbert phase shift.

bias current of 70 mA, which is 1.24 times the threshold current of 56.4 mA, respectively. The mean intensity has been set to zero. In Fig. 3(a), the feedback is weak and the small fluctuations are due to the spontaneous emission and the feedback. As the feedback strength increases, the fluctuations become larger and spontaneous emission could be ignored [Figs. 3(b), 3(c)]. These figures do not give us much insight, apart from the obvious increase in fluctuation amplitude with feedback strength. However, if we go further and look at the phase space of the intensity vs the Hilbert phase shift for one round-trip time τ for three different feedback strengths [Figs. 3(d)–3(f)], we immediately see the change of the behavior of the laser with increasing feedback strength, resulting in creation of external cavity modes. With very small feedback [Fig. 3(d)], the phase varies continuously in a big cluster distributed from 0 to 6π . As the feedback strength increases, the cluster starts splitting into discrete ones at multiples of 2π [Fig. 3(e)] and these clusters finally become very distinguishable [Fig. 3(e)]. Thus, the Hilbert phase reveals a dramatic change in the laser dynamics with the change in the feedback, which was not evident from the intensity time series displayed in Figs. 3(a)–3(c).

In Figs. 4(a), 4(b), and 4(c), we show numerical simulations with $P=1.24$ and $R=0.01$, 0.076 and 0.123, respectively. We ignore the spontaneous emission term $F_E(t)$ because the bias current is much above threshold. Adding the $F_E(t)$ term in the simulations does not alter the time series. This is to be expected, since the spontaneous emission noise is negligible at such high pumping levels. All other laser parameters are maintained same as in the previous computa-

tions. The three figures show a very similar behavior when compared to the experimental observations displayed in Figs. 3(a), 3(b), and 3(c), respectively. The ratios between the three intensity amplitudes match those of the experiments too. In Figs. 4(d)–4(f), three corresponding phase space trajectories show similar cluster splitting transitions for the three feedback strengths.

In conclusion, the semiconductor laser with optical feedback in different regimes has been studied using Hilbert phase analysis of the real intensity time series both for the experimental and numerical simulation data. The formation and result of interaction of external cavity modes of the feedback system is demonstrated by the Hilbert phase shift which

is otherwise not obvious from the intensity time series. In general, the Hilbert phase shift is constant at 2π for periods which are multiples of the external round-trip time. The small fluctuations of this phase shift, as well as the 2π jumps, show deviations from a truly periodic signal. The zero-phase cluster helps us identify the dropout phenomenon. Thus, the analytic signal of an intensity time series proves to be a very powerful way to extract information on the phase relationships between coupled degrees of freedom from the original data which is otherwise not evident.

We gratefully acknowledge support from the Office of Naval Research (Physics) and thank Ingo Fischer, Sebastian Wieczorek, and Edward Ott for helpful discussion.

-
- [1] C. Risch and C. Voumard, *J. Appl. Phys.* **48**, 2083 (1977).
 - [2] D. Lenstra, B.H. Verbeek, and A.J. den Boef, *IEEE J. Quantum Electron.* **QE-21**, 674 (1985).
 - [3] R. Lang and K. Kobayashi, *IEEE J. Quantum Electron.* **QE-16**, 347 (1980).
 - [4] C.H. Henry and R. Kazarinov, *IEEE J. Quantum Electron.* **QE-22**, 294 (1986).
 - [5] J. Mørk, J. Mark, and B. Tromborg, *Phys. Rev. Lett.* **65**, 1999 (1990).
 - [6] T. Sano, *Phys. Rev. A* **50**, 2719 (1994).
 - [7] G.H.M. van Tartwijk, A.M. Levine, and D. Lenstra, *IEEE J. Sel. Top. Quantum Electron.* **1**, 466 (1995).
 - [8] A. Hohl, H.J.C. van der Linden, and Rajarshi Roy, *Opt. Lett.* **20**, 2396 (1995).
 - [9] I. Fischer *et al.*, *Phys. Rev. Lett.* **76**, 220 (1996).
 - [10] M. Giudici *et al.*, *Phys. Rev. E* **55**, 6414 (1997).
 - [11] G. Huyet *et al.*, *Europhys. Lett.* **40**, 619 (1997).
 - [12] T. Heil, I. Fischer, and W. Elsässer, *Phys. Rev. A* **58**, R2672 (1998).
 - [13] G. Vaschenko *et al.*, *Phys. Rev. Lett.* **81**, 5536 (1998).
 - [14] A. Hohl and A. Gavrielides, *Phys. Rev. Lett.* **82**, 1148 (1999).
 - [15] D. Sukow *et al.*, *Phys. Rev. A* **60**, 667 (1999).
 - [16] A. Prasad *et al.*, *J. Opt. B: Quantum Semiclassical Opt.* **3**, 242 (2001).
 - [17] C. Masoller, *Phys. Rev. Lett.* **88**, 34102 (2002).
 - [18] D. Gabor, *J. IEE (London)* **93**, 429 (1946); M. Born and E. Wolf, *Principles of Optics*, 7th ed. (Cambridge University Press, Cambridge, 1999), pp. 557–562.
 - [19] T. Yalçinkaya and Y.C. Lai, *Phys. Rev. Lett.* **79**, 3885 (1997); N. Huang *et al.*, *Proc. R. Soc. London Ser. A* **454**, 903 (1998); I. Wallace *et al.*, *Phys. Rev. A* **63**, 013809 (2000); D. Deshazer *et al.*, *Phys. Rev. Lett.* **87**, 044101 (2001).